行政院國家科學委員會補助專題研究計畫成果報告

利用酵母菌囊狀泡傳送系統分析
及探討新發現人體基因的功能

計畫類別：■個別型計畫　　□整合型計畫

計畫編號：NSC89－2318－B002－001－M51

執行期間：88年8月1日至89年7月31日

計畫主持人：李芳仁副教授

共同主持人：

本成果報告包括以下應繳交之附件：

- □赴國外出差或研習心得報告一份
- □赴大陸地區出差或研習心得報告一份
- □出席國際學術會議心得報告及發表之論文各一份
- □國際合作研究計畫國外研究報告書一份

執行單位：國立台大醫學院分子醫學研究所

中　華　民　國　89 年 10 月 13 日

ARL4, an ARF-like Protein that is Developmentally Regulated and Localized to Nuclei and Nucleoli

Ching-Yi Lin[1,#], Pei-Hsin Huang[2,#], Wei-Li Liao[1], Hwai-Jong Cheng[2], Chun-Fang Huang[1], Jer-Cheng Kuo[1], Walter A. Patton[3,+], Donald Massenburg[3,$], Joel Moss[3], and Fang-Jen S. Lee[1]*

[1]Institute of Molecular Medicine, and [2]Institute of Pathology, College of Medicine, National Taiwan University, Taipei, Taiwan, R.O.C.; [3]Pulmonary-Critical Care Medicine Branch, NHLBI, National Institutes of Health, Bethesda, MD 20892-1590, U.S.A.

*To whom correspondence should be addressed: 7 Chung Shan South Road, Taipei, Taiwan. Phone: 886-2-2397-0800 ext. 5730. Fax: 886-2-2395-7801, E-mail: fangjen @ ha.mc.ntu.edu.tw

# These authors contributed equally to this work.

+Present address: Department of Chemistry, Lebanon Valley College, 101 N. College Ave., Annville, PA 17003.

$ Present address: 9034 Washington Dr., Apt. 2B, Des Plaines, IL 60016

Running Title: ARL4 is Developmentally Regulated and Localized to the Nucleus

Abbreviations: ARF, ADP-ribosylation factor; hARF, human ARF; ARL, ARF-like protein; ER, endoplasmic reticulum; GEP, guanine nucleotide-exchange protein; GST, glutathione-S-transferase; NLS, nuclear localization signal; PCR, polymerase chain reaction; dpc, days post-coitus.

ABSTRACT

ADP-ribosylation factors (ARFs) are highly conserved ~20-kDa guanine nucleotide-binding proteins that participate in both exocytic and endocytic vesicular transport pathways via mechanisms that are only partially understood. Although several ARF-like proteins (ARLs) are known, their biological functions remain unclear. To characterize its molecular properties, we cloned mouse and human ARL4 (*mARL4* and *hARL4*) cDNA. The appearance of mouse ARL4 mRNA during embryonic development coincided temporally with the sequential formation of somites and the establishment of brain compartmentation. Using ARL4-specific antibody for immunofluorescence microscopy, we observed that endogenous mARL4 in cultured Sertoli and neuroblastoma cells was mainly concentrated in nuclei. When expressed in COS7 cells, ARL4 - T34N mutant, predicted to exist with GDP bound, was concentrated in nucleoli. Yeast two-hybrid screening and *in vitro* protein-interaction assays showed that hARL4 interacted with importin-α through its C-terminal NLS region and that the interaction was not nucleotide-dependent. Like ARL2 and 3, recombinant hARL4 did not enhance cholera toxin-catalyzed auto-ADP-ribosylation. Its binding of GTPγS was modified by phospholipid and detergent, and the N-terminus of hARL4, like that of ARF, was myristoylated. Our findings suggest that ARL4, with its distinctive nuclear/nucleolar localization and pattern of developmental expression, may play a unique role(s) in neurogenesis and somitogenesis during embryonic development and in the early stages of spermatogenesis in adults.

Key words: ADP-ribosylation factors, spermatogenesis, neurogenesis, somitogenesis, importin-α.

INTRODUCTION

The Ras superfamily of ~ 20-kDa guanine nucleotide-binding proteins (or GTPases) contains more than 100 gene products which have been grouped into five subfamilies, i.e., the Ras, Rab, Rho, Ran, and ARF families. The ARF (ADP-ribosylation factor) family, which is most different from the other groups, comprises at least six ARFs and six ARF-like (ARL) proteins (reviewed in Refs. 1 and 2). Although ARFs and ARLs are very similar in amino acid sequences, most ARLs, but not ARL1, apparently do not activate the cholera toxin ADP-ribosyltransferase. They differ also from ARFs in having demonstrable GTPase activity and different conditions that favor guanine nucleotide binding. Both ARFs and ARLs are widely distributed in eukaryotic organisms from yeast to human, consistent with evolutionary conservation of their biological functions.

ARFs play an important role in intracellular membrane trafficking, although there remains much to be learned. The biological functions of ARLs are still unclear, although some are expressed in a tissue- and/or differentiation-specific pattern (3-7). ARL1 was localized in the Golgi complex of normal rat kidney cells (8) and *S. cerevisiae* (9), consistent with a function in vesicular trafficking. Unlike the lethal phenotype of double null alleles of *arf1* and *arf2*, however, knock-out of the yeast ARL1 gene was not lethal (9). Expression of rat ARL4 was reported to be cell differentiation-dependent (4). Its role in adipocyte metabolism and sperm production was suggested (10) and nuclear localization of transiently expressed protein was demonstrated (11).

To obtain additional clues to its physiological role(s), we investigated the expression, subcellular localization, and biochemical properties of ARL4. As reported here, mouse ARL4 (mARL4), which is abundant in testis, is developmentally regulated during mouse embryogenesis. The mARL4 mRNA appears transiently, progressing in a rostro-caudal direction in day-8.5 to day-10.5 embryos, which coincides temporally with the appearance of somitomeres in the same locations. Endogenous mARL4 in Sertoli (TM4) and neuroblastoma (Neuro 2A) cells was mainly localized in

nuclei. When expressed in COS7 cells, ARL4 -T34N, a mutant predicted to be GDP-bound, was localized to nucleoli. This may be the first report of a small GTPase localized in nucleoli in a nucleotide-dependent manner. Data from yeast two-hybrid and *in vitro* protein interaction analyses revealed that hARL4 interacted with the NLS-receptor, importin-α, through a bipartite nuclear localization signal (NLS) in its C-terminal region and that this interaction was not nucleotide-dependent. To our knowledge, no other small GTPase has been implicated in the regulation of somite development. The specific spatial and temporal expression of mouse *ARL4* mRNA in the central nervous system during later embryonic stages suggests that ARL4 might also be involved in neuronogenesis or cortical histogenesis. Thus, ARL4 may have a physiological role(s) in vertebrate somite formation, and central nervous system differentiation, as well as in the early events of gametogenesis.

EXPERIMENTAL PROCEDURES

Isolation of Mouse and Human ARL4 cDNA --- Mouse ARL4 cDNA was synthesized by polymerase chain reaction (PCR) from a mouse λgt11 cDNA library. PCR-based cloning methods were used to obtain cDNA segments, from which a composite sequence of the full-length coding region was assembled (12). A probe composed of degenerate oligonucleotides (ARL-R1, and ARL-R2)(Table 1) corresponding to part of the consensus sequences WDVGGQE and KLRPLWK in human and rat ARL4 was used to screen a mouse λgt11 cDNA library (Clontech) in the one-site-specific PCR to capture 3' and 5' ends of mouse ARL4 cDNA as previously described (9). All PCR products were purified, subcloned, and sequenced by the dideoxy chain-termination method (13). The nucleotide sequence of mouse ARL4 has GenBank accession number U76546. Human ARL4 cDNA was isolated by same procedures. The identical nucleotide sequence was deposited by Kim et al. (GenBank accession number U73960).

Northern Analyses --- Blots with RNAs from adult mice and mouse embryos at several stages of development (Clontech) were processed for hybridization with mARL4- specific probes as described previously (12). A blot with samples of poly (A)$^+$RNA (2 μg) from testes of 5, 10, 15, 20, 25, 30 and 60 day old rats was kindly provided by Dr. Ian Okazaki (NIH). TM4 (Sertoli) and MA10 (Leydig) cells were grown and harvested as described (14, 15). Total RNA was extracted and reverse-transcribed using a reverse transcriptase kit (Gibco). The identity of the RT-PCR product was confirmed by Southern blotting with an mARL4 cDNA probe.

In Situ RNA Hybridization --- mARL4 RNA probes were prepared from pCRII-mARL4 constructed by PCR amplification of the adult mouse ARL4 cDNA and cloning of the product into the pCRII vector. *In situ* hybridization using digoxigenin(dig)-labelled RNA probes was performed as described by Cheng et al. (16). Briefly, 14-μm cryo-sections of day-12.5, -14.5, -17.5, or -19.5 mouse embryos were incubated serially with 6% H_2O_2, 1xPBT (PBS with 0.1% Tween-20), protease K, and 4% paraformaldehyde for fixation. Prehybridization was performed at 70^{o}C for 2 hr, followed by overnight hybridization at 70^{o}C with the dig-labelled probe (1μg/ml) in hybridization buffer (50% formaldehyde, 5xSSC, and 1% SDS containing yeast tRNA (50 μg/ml) and heparin (50 μg/ml)). After three stringent post-hybridization washes with 50% formaldehyde/ 2xSSC, slides were incubated (2 h, room temperature) with anti-digoxigenin antibody conjugated with alkaline phosphatase (Boehringer Mannheim) diluted 1:2000, and colorized by incubation with substrate NBT/BCIP (nitro blue tetrazolium chloride/ 5-bromo-4-chloro-3-indolyl-phosphate). Inspection and photography were performed with an Olympus microscope. *In situ* RNA hybridization with whole mounted embryos was performed as described by Cheng and Flagnan (17).

Expression and Purification of Recombinant Proteins --- The entire open reading frame of human ARL4 was obtained by PCR, using primers that incorporated unique *Nde*I and *Bam*HI sites, respectively, at the initiating methionine and 6 bp downstream from the stop codon. For the preparation of the His-tagged fusion protein, the hARL4 PCR product was cloned into the

expression vector pET15b (Novagen), yielding pET15b-His-hARL4. For the nonfusion protein, the hARL4 PCR product was digested with *Nde*I and *Bam*HI, purified, and annealed to expression vector pT7/Nde (18), yielding pT7-ARL4, which was used to transfect BL21 (DE3)(9). Cell pellets were harvested and His-tagged fusion protein was isolated on Ni^{2+}-NTA resin (Qiagen, Chatsworth, CA) by standard methods. The purity of the His-tagged hARL4 was assessed by SDS-PAGE.

Generation of ARL4 Antisera and Immuno-analyses --- Rabbits were immunized with keyhole limpet hemocyanin-conjugated synthetic peptide LRNSLSLSEIEKLLAMGC (peptide B), corresponding to the residues 138-154 of hARL4. Antibodies (ARL4-B) were affinity-purified on immobilized, recombinant hARL4. Western analysis and immunoprecipitation were performed according to the procedures of Harlow and Lane (19).

Fractionation by Differential Centrifugation --- Nuclear (N), crude cytosol (C), and membrane (M) fractions were prepared as described previously (20, 21). Briefly, confluent TM4 cells were scraped and homogenized in HES buffer (20 mM HEPES, pH 7.4, 1 mM EDTA, 250 mM sucrose) plus 1 mM phenylmethylsulfonyl fluoride (PMSF) and a mixture of protease inhibitors (leupeptin, aprotinin, chymostatin, antipain, and pepstatin, each 1 μg/ml) at 4 °C by 10 strokes in a ball-bearing homogenizer. The cell lysate was centrifuged at 400 x g for 10 min to eliminate unbroken cells, nuclei, and cell debris. The supernatant was centrifuged (150,000 x g, 1 h) at 4 °C to generate cytosolic (C) and membrane (M) fractions. To obtain the nuclear fraction, cell pellet containing unbroken cells, nuclei, and cell debris was dispersed in 1 ml of TBS (Tris-buffered saline), transferred to an Eppendorf tube and centrifuged for 15 sec in a microfuge. TBS was removed and the pellet was suspended in 400 μl of cold buffer A (10 mM HEPES, pH 7.9, 10 mM KCl, 0.1 mM EDTA, 0.1 mM EGTA, 1 mM DTT, 0.5 mM PMSF) by gentle pipetting in a yellow tip. The cells were allowed to swell on ice for 15 min, after which 25 μl of a solution

containing 10 % Nonidet NP -40 were added and the tube was vigorously vortexed for 10 sec. The homogenate was centrifuged for 30 s in a microfuge, and the nuclear pellet (N) was collected (21).

Cell Culture and Transient Transfection --- Sertoli TM4 cells were grown at at 37 °C on glass coverslips (18-mm diameter) in 12-well dishes for 16 h before processing at room temperature. Mouse neuroblastoma cells, Neuro 2a (ATCC: CCL-131), were grown in Dulbecco's modified Eagle's medium (DMEM, GIBCO), supplemented with 10 % fetal bovine serum, 2 mM glutamine and 100 units/ml each of penicillin and streptomycin. The cells were subcultured by trypsinization [0.05 % (wt/vol) trypsin, with 1 % EDTA], and plating in growth medium in a humidified 5 % CO_2 incubator at 37°C every 2 to 3 days. The cDNA fragments of hARL4 were fused in-frame to the C-terminus of GFP by subcloning into the *Eco*RI and *Sal* I sites of pEGFP-C2 (Clontech). COS7 (ATCC: CRL-1651) cells were seeded on coverslips 16 h before transfection with the aid of Lipofectamine (Life Technologies, Inc.). Freshly prepared solution A (2 μg of plasmid DNA in 50 μl DMEM) and solution B (6 μl Lipofectamine in 50μl DMEM) were gently mixed for 30 min at room temperature, added to 400 μl of DMEM and incubated with cells for 6 h at 37°C. Additional growth medium with 20 % FBS (500 μl) was then added without removing the transfection mixture. Medium was replaced with fresh growth medium the day after transfection, and cells were harvested 30 to 36 h later for analysis.

Indirect Immunofluorescence Staining and Immunohistochemistry --- Cells were fixed with 4% paraformaldehyde in PBS-Ca^{2+}-Mg^{2+} (0.6 mM $CaCl_2$ and 0.5 mM $MgCl_2$ in 1x PBS) for 15 min, incubated with 0.1% Triton X-100 and 0.05% SDS in PBS-Ca^{2+}-Mg^{2+} for 4 min, and in the same buffer containing 0.2% BSA for an additional 15 min, followed by incubation with primary antibodies; i.e., affinity purified anti-hARL4-peptide, mouse anti-p58 (Sigma), mouse anti-β-COP

(Sigma), or mouse anti-C23 (nucleolin, Santa Cruz) in the same blocking solution for 40 min. After three washes with PBS-Ca^{2+}-Mg^{2+}, cells were incubated with second antibody, Alexa 594-conjugated anti-rabbit IgG antibody or Alexa 488-conjugated anti-mouse IgG antibody (Molecular Probes), washed three times with PBS-Ca^{2+}-Mg^{2+}, mounted on Mowiol (supplemented with Hoescht 33258), and examined with a Zeiss Axiophot equipped for epifluorescence according to standard procedures (22). Primary antibodies previously depleted of anti-ARL4 activity by incubation with purified recombinant hARL4 were used as control. Immunohistochemistry was performed using an avidin-biotin system, the ABC Vectastain Elite kit (Vector Laboratories, Burlingame, CA). Representative, mouse embryos were fixed in 4% paraformaldehyde and processed for OCT block preparation. 5-mm cryostat sections of coronally positioned 14-dpc embryos were collected. After several rinses with phosphate-buffered saline, pH7.4 (PBS), endogenous peroxidases were quenched by adding 6% hydrogen peroxide in PBS for 15 min at room temperature. After washing with PBS, sections were treated with 20% normal goat serum for 30 min, washed with PBS, incubated with the anti-ARL4 antibody for 1 h at room temperature, and then washed with PBS. Biotinylated goat anti-rabbit antibodies diluted 1:200 in PBS were added to sections for 1 h at room temperature, followed by washing with PBS and addition of 0.05% 3,3'-diaminobenzidine tetrahydrochloride. Color development was monitored and stopped by dilution with water. Sections were dried, mounted, and inspected by light microscopy (Olympus company).

Yeast Two-hybrid Screen and Assay --- Yeast strains (L40), plasmids (pBTM116 and pVP16), and library for the yeast two-hybrid screen were obtained from Dr. H. Shih. The genotype of the *Saccharomyces cerevisiae* reporter strain L40 is *MATa trp1 leu2 his3 LYS2::lexA-HIS3 URA3::lexA-lacZ* (23). Yeast strains were grown at 30 °C in rich medium (1% yeast extract, 2% Bacto-peptone, 2% glucose) or in synthetic minimal medium with appropriate supplements. Full length wild type hARL4 cDNA was generated using 5' (sense) primer ARL4A, and 3' (antisense) primer ARL4B (Table 1). Replacement of Thr34 with Asn (T34N) or Gln79 with Leu

(Q79L) were accomplished using a two step PCR technique as described (22). The 5' (sense) mutagenic primer ARL4C and the antisense mutagenic primer ARL4D were used to generate hARL4-Q79L. The 5' (sense) mutagenic primer ARL4E and the antisense mutagenic primer ARL4F were used to generate hARL4-T34N. The point mutation is underlined in oligonucleotide sequences (Table 1). To generate ARL4-dC (NLS-deleted mutant) with deletion of 11 C-terminal amino acids (positions 190 through 200) that include the putative nuclear localization signal (10), PCR amplification was used with primer ARL4A and the mutagenic 3'-end anti-sense oligonucleotide primer ARL4G. Plasmids pLexA-ARL1, pLexA-ARL3, pLexA-ARL4, pLexA-ARL4-Q79L, pLexA-ARL4-T34N, and pLexA-ARL4-dC, constructed, respectively, by inserting a PCR-generated fragment of the ARL1, ARL3, ARL4, ARL4-Q79L, ARL4-T34N, or ARL4-dC cDNA into the *EcoR*I site of the pBTM116 plasmid, were used to express the ARL as a fusion protein with the DNA-binding domain of LexA.

For two-hybrid screening, the yeast reporter strain L40, which contains the reporter genes *lac*Z and *HIS3* downstream of the binding sequences for LexA, was transformed with pLexA-ARL4-Q79L and a human testis pACT2 cDNA library (Clontech) by the lithium acetate method (24), and subsequently treated as described (23). Double transformants were plated with synthetic medium lacking histidine, leucine, tryptophan, uracil, and lysine. Plates were incubated at 30 °C for 3 days. His^+ colonies were patched on selective plates and assayed for β-galactosidase activity by a filter assay (23). Plasmid DNA was prepared from colonies displaying a $HIS^+/lacZ^+$ phenotype by electrotransformation of HB101 cells and used to re-transform the L40 strain containing the appropriate pLexA-ARL1, pLexA-ARL3, pLexA-ARL4, pLexA-ARL4-Q79L, pLexA-ARL4-T34N, pLexA-ARL4-dC, and pLexA-lamin, to test for specificity. For assay of β -galactosidase activity, transformants were grown in histidine-containing medium, lysed, and assayed as described (23).

In vitro Interaction of ARL4 and Importin-α --- Recombinant human ARL4 mutants (ARL4-Q79L, ARL4-T34N, and ARL4-dC) were PCR-amplified from the *Nde*I site upstream of the initiator methionine codon. PCR fragments were ligated into the pT7Blue Blunt vector (Novagen). The pT7Blue (ARL4s) plasmids were digested with *Nde*I and *BamH*I and the ARL4 fragments were ligated in-frame to the pET-15b expression vector (Novagen). To synthesize importin-α as an N-terminal GST fusion protein, importin-α cDNA was amplified by PCR using primers containing *Not*I sites at both 5'- and 3'-ends. After ligation into pT7Blue Blunt vector, the *Not*I/*Not*I fragment was subcloned into the same sites of GST fusion vector pGEX-4T1 (Pharmacia Biotech Inc.) to generate pGEX-importin-α. Transformed *E. coli* strain BL21 were grown and recombinant protein was prepared as previously described (9). The soluble fraction of *E. coli* expressing GST or GST-importin-α was incubated with glutathione-Sepharose 4B beads (Amersham Pharmacia biotech) for 30 min at room temperature. The beads were then washed four times with PBS, and finally suspended in PBS. GST and GST-importin-α immobilized on glutathione-Sepharose beads were quantified by SDS-PAGE with Coomassie blue staining.

Each hARL4 construct was expressed in *E. coli*, and 750 μl of each soluble fraction were incubated at 4°C for 1 h with 10 μg of GST or GST-importin-α immobilized on glutathione-Sepharose beads. After washing five times with ice-cold washing buffer (25 mM Tris-HCL, pH 8.0, 100 mM NaCl, 10 mM $MgCl_2$, 1 mM dithiothreitol), beads plus 25 μl of SDS sample buffer were boiled for 10 min and a 15-μl sample of each supernatant was subjected to SDS-polyacrylamide gel electrophoresis in 12% gel along with a 7.5-μl sample of each original soluble fraction. Bound proteins were analyzed by immunoblotting.

Expression and Detection of Myristoylated ARL4 --- To produce myristoylated proteins, BL21(DE3) competent bacteria were co-transfected with pT7-ARL4 and pACYC177/ET3d/yNMT, which encodes yeast (*S. cerevisiae*) *N*-myristoyltransferase (25), and selected for both ampicillin and kanamycin resistance. [9,10(n]-^{3}H)myristic acid (1mCi/ml in ethanol, Amersham, Inc.) was added to a final concentration of 30 μCi/ml and the cultures were further treated as described (26). Proteins separated by SDS-PAGE were transferred electrophoretically to Immobilon-P membranes (Millipore). Incubation with indicated antibodies was carried out in phosphate-buffered saline (pH 7.4) containing 0.1% Tween 20 and 5% dried skim milk at room temperature for 60 min. Bound antibodies were detected with the ECL system (Amersham Corp.) according to the manufacturer's instructions.

CTA-catalyzed ADP-ribosylation and Nucleotide Binding Assay ---Samples (5 μg) of purified His-tagged -hARL4 or -yARF1 fusion proteins were tested for their ability to stimulate cholera toxin-catalyzed auto-ADP-ribosylation (27). Binding of GTPγS to purified recombinant hARL4 was determined by a filtration method (22) with minor modification (9). Unless otherwise specified, 3 μg of His-tagged hARL4 were incubated at 30°C in 20 mM HEPES (pH 7.5), 100 mM NaCl, 1 mM dithiothreitol, 1 mM EDTA, 0.5 mM $MgCl_2$, and 4μM [^{35}S]GTPγS (Amersham, >1000Ci/mmol) containing bovine serum albumin (BSA), 20 μg/ml, without or with the indicated lipids, in a final volume of 50 μl. Duplicate or triplicate samples were transferred to 2 ml of ice-cold 20 mM Tris-Cl, pH 7.4, 100 mM NaCl, 10 mM $MgCl_2$, 1 mM dithiothreitol before rapid filtration on 0.45-μm HA filters (Millipore, Bedford, MA). Nucleotide bound to the fusion protein was quantified by scintillation counting.

RESULTS

Developmentally Regulated Expression of mARL4 --- mARL4 mRNA was much more abundant in testis than in other adult mouse tissues (Fig. 1A). A prominent ~ 1.4-kb transcript along with a lesser one of ~ 4.0 kb was observed in mouse tissues. On Northern blot analysis of mouse embryos at different stages of development, the level of mARL4 mRNA was highest on embryonic day 7 and was 90% lower by day 11 (Fig. 1B). Northern blot analysis of whole testis preparations collected from prepubertal (5 and 10 days), early pubertal (15 days), mid-pubertal (20 and 25 days), late pubertal (30 days), and adult (60 days) rats revealed a major rat ARL4 mRNA of 1.4 kb that was first detectable in mid-pubertal testis and was more abundant in the mature 30 and 60 day-old testis possessing fertilizing activity (Fig. 1C). *In situ* hybridization with frozen sections of testis and epididymis from 3- and 6-month old mice identified mARL4 RNA mainly localized in the basal region of seminiferous tubules (i.e., spermatogonia/ spermatocytes and Sertoli cells); it was not detected in the androgen-producing Leydig cells (data not shown), as reported by Jacobs et al. (10). Similarly, in cultured cell lines, RT-PCR showed that Sertoli cells (TM4), but not Leydig cells (MA10), had mARL4 transcripts, consistent with the results of *in situ* hybridization, although, combined RT-PCR and Southern analysis, did reveal small amounts of mARL4 mRNA in the Leydig cell line (data not shown).

In situ Hybridization Analysis of ARL4 RNA in Mouse Embryos --- Abundant mARL4 mRNA was detected in 7-dpc (days post-coitus) mouse embryos (Fig. 1B). *In situ* hybridization of mouse embryos at 8-10 dpc and of tissue-sections of embryos at later stages was performed to determine whether mARL4 is expressed in tissue-specific manner during embryonic development. mARL4 mRNA was prominent at the earliest timepoint analyzed, day-8.5 at the 10-12 somite stage (Fig. 2A), localized specifically in pairs of somites and at the junction of forebrain and midbrain (Fig. 2A, red and black arrows, respectively). In 9.0-dpc embryos, mARL4 mRNA was present in more caudal somites, coinciding with the sequential formation of new somites (Fig. 2B; red arrow). At the 25-29 somite stage (day-9.5 embryos), mARL4 mRNA was concentrated at the junction of

midbrain and hindbrain (Fig. 2C, arrowhead) and in the caudal somites (Fig. 2C; red arrow); it had disappeared from the first 10 –12 pairs of somites and the forebrain-midbrain junction.

Later in embryonic development (Fig. 3A and D), mARL4 mRNA was detected in the neuronal stoma around the central canal, the dorsal and ventral horns of the spinal cord, and the root ganglia (day-14.5 embryo). It was still present in the spinal cord and root ganglia of day-16.5 embryos (Fig. 3B and E). In day-14.5 to -17.5 embryos, the brain parenchyma contained less mARL4 mRNA than did the spinal cord. A prominent zone of mARL4 mRNA was detected, however, in the neopallial cortex of the day-17.5 embryo (Fig. 3C). mARL4 mRNA decreased with maturation and was undetectable in the spinal cord of the neonatal mouse, although trace amounts were still discernible in the brain parenchyma (data not shown).

Subcellular Localization of ARL4 --- To identify the intracellular location of the ARL4 protein, we generated ARL4-specific antibodies against a unique peptide sequence (residues 138-154) of human ARL4. Predicted amino acid sequences of human and mouse ARL4 differ only at position 14 (data not shown). The affinity-purified antibodies proved to be sensitive and specific for detection of both human and mouse ARL4 proteins. Immunoblotting with this antiserum detected ARL4 in low nanogram amounts, while no reaction was detected with 100 ng of other recombinant ARLs (Fig. 4A).

To assess the subcellular distribution of ARL4 in mouse Sertoli TM4 cells, homogenates were fractionated by differential centrifugation. Nuclear (N), membrane (M), and cytosol (C) fractions were separated and ARL4, PCNA (proliferating cell nuclear antigen), and tubulin (cytoplasmic marker) in subcellular fractions were identified by Western blot analysis (Fig. 4B). Using affinity-purified anti-ARL4 antibodies, endogenous ARL4 was detected in the nuclear fraction, whereas immuno-precipitated ARL1 was in the cytoplasmic fraction (Fig. 4B). ARL3 was not detected in the TM4 cells. The specific ARL1, ARL3, and ARL4 antibodies used did not cross-react with other ARLs. Immuno-detection of ARL4 was abolished by prior incubation of the antiserum with

recombinant ARL4 (data not shown). By immunofluorescence microscopy, endogenous mARL4 of Sertoli TM4 and neuroblastoma (Neuro 2a) cells was distributed mainly over the nucleus in a fine punctate pattern (Fig. 4C). No immunoreactivity was detected after incubation of antibody ARL4-B with purified recombinant ARL4 (Fig. 4C, e) or with preimmune serum (not shown). Nuclei were stained with the DNA-binding dye H33258 (Fig. 4C, b, f and j) and Golgi with anti-β-COP antibodies (Fig. 4C, c, g, and k).

We have tried, thus far without success, to demonstrate nuclear localization of ARL4 in mouse fetal tissues. In the day-14 embryo, only weak staining was observed in the spinal cord and root trunks by immunohistochemistry, and none in the adjacent tissues derived from myotome and sclerotome (Fig. 4D). This is consistent with the low level of ARL4 mRNA in the day-11 mouse embryo (Fig. 1B), and makes it difficult to establish mARL4 localization in nuclei.

Two-hybrid Interaction of Importin-α with ARL4 C-terminal Nuclear Localization Signal NLS --- To identify molecules that might act as down-stream effectors of ARL4, we used plasmid pLexA-ARL4-Q79L to express the putatively constitutively active mutant of ARL4 (ARL4-Q79L) as bait in a yeast two-hybrid screen of human testis cDNA library (23). Plasmids that were associated with β-galactosidase production were identified from a screen of approximately 4 x 10^6 colonies. The DNA sequence of each library insert was determined and eight distinct genes were chosen for further analysis. One of these, importin-α (karyopherin alpha 2; accession number NM_002266)(28, 29), was further characterized to support the observations on ARL4 localization. Five different fragments (residues 1-530, 135-530, 152-350, 233-530, and 235-530) of importin-α (total of 530 amino acids) interacted with pLexA-ARL4-Q79L. Because ARL4 contains a putative bipartite NLS (K^{188}RRKMLRQQKKKR^{200}) at its C-terminus (Fig. 5A), we constructed an NLS-deleted ARL4 mutant (ARL-dC) to test whether interaction of hARL4 and importin-α is dependent on this sequence. We also constructed wild type ARL4 and ARL4-T34N (predicted to

be GDP-bound mutant) to test whether interaction of hARL4 and importin-α is nucleotide-dependent. All of the LexA fusion ARL proteins were expressed in yeast and detected by antibodies against LexA or against specific ARLs (Fig 5B). In yeast two-hybrid assay, transformants containing interacting proteins that transactivate two reporter genes, *HIS3* and *LacZ*, exhibit β-galactosidase activity and can grow on minimal medium lacking histidine. As illustrated in Figure 5C, LexA-ARL4, LexA-ARL4-Q79L, and LexA-ARL4-T34N, but not LexA-ARL4-dC, LexA-ARL1, or LexA-ARL3, interacted with the Gal4AD-importin-α fusion protein and activated the reporter genes.

To confirm that the interactions between ARL4 and importin-α are direct, an *in vitro* GST pull-down assay was used. Recombinant His-tagged hARL4 and its mutants were produced in *E. coli*, and the soluble bacterial proteins were incubated with immobilized GST-importin-α *in vitro*. As shown in Fig.5D, recombinant GST-importin-α, but not GST, adsorbed significant amounts of ARL4, ARL4-Q79L, and ARL4-T34N, whereas no binding of ARL4-dC or ARL1 was detected. Binding of ARL4 and the two mutants (expected to exist largely in GTP- or GDP-bound forms) was not grossly different.

Nucleolar Localization of ARL4-T34N mutant --- Although transient expression of hARL4 had shown its nuclear localization (11), we wanted to examine further whether the subcellular localization of ARL4 was dependent on GTP or GDP binding. COS7 cells transiently expressing GFP-ARL4, -ARL4-Q79L, -ARL4-T34N, and -ARL4-dc were inspected by fluorescence microscopy (Fig. 6A). ARL4 appeared to be located in nuclei and partially in nucleoli (Fig. 6A, a-c; arrows). ARL4-T34N, but not ARL4-Q79L, appeared to be more concentrated in nucleoli (Fig. 6A, i-k; arrows). The nucleolar localization of ARL4-T34N was confirmed by coimmunostaining with nucleolin, a marker for nucleoli. ARL4-T34N was colocalized with nucleolin, confirming its

nucleolar localization (Fig 6A, q-t). ARL4-dC, not seen in nuclei, was in part co-localized with the Golgi marker p58 (Fig 6A, o and p). Subcellular distribution of transiently expressed hARL4 and its mutants in homogenates of COS7 cells was also examined. ARL4, ARL4-Q79L, and ARL4-T34N were detected mainly in the nuclear fraction with very little in the membrane fraction (Fig. 6B). ARL4-dC, however, appeared mainly in the membrane fraction, confirming the results of fluorescence microscopy.

Functional Properties of ARL4 Protein --- The hARL4 fusion protein, like ARL2 and ARL3, failed to stimulate auto ADP-ribosylation of the cholera toxin A1 protein (data not shown). It did bind GTPγS in a concentration-dependent manner that reached a steady state within 60 min at 30°C. Phospholipids that increased GTPγS binding by hARF1, however, markedly decreased binding by hARL4 (Fig. 7). To determine whether hARL4 could be myristoylated, hARL4, hARL1, and yARL3 were co-expressed in *E. coli* with yeast N-myristoyltransferase. As shown in Figure 8, hARL4 was myristoylated as was hARL1, which has been reported (9). yARL3, previously shown not to be myristoylated (26), served as a negative control. Thus, the biological function of ARL4, like those of ARFs and other proteins, may be influenced by myristoylation.

DISCUSSION

We have characterized the expression, subcellular localization, and biochemical properties of a highly conserved small GTPase, ARL4. RNA blot hybridization revealed more than one species of ARL4 mRNA, which might serve different biological functions in different cells. The existence of multiple mRNAs has been reported also for human ARL1 (7), ARL3 (5), and ARFs (reviewed in Refs. 1 and 2). Our data clearly indicate that the expression of mARL4 mRNA is developmentally

regulated and are consistent with involvement of the protein in early events of spermatogenesis, somitogenesis, and the embryogenesis of the murine central nervous system. By indirect immunofluorescence and biochemical techniques, we show that localization of ARL4 in nucleoli is influenced by nucleotide binding.

ARL4 mRNA, which was detected in numerous adult organs, was most abundant in the spermatogonia and/or Sertoli cells of adult testis. No reactivity was detected in the epididymis by *in situ* hybridization, suggesting that ARL4 is not involved in the activation of motility or the maturation of spermatids induced by the ciliated epithelium of epididymis. The mRNA for rat ARL4, which differs in only one amino acid from mouse ARL4, was reported to be abundant in testis and 3T3-L1 adipocytes (10).

In mouse embryo, the pattern of appearance of ARL4 mRNA proceeding in a rostro-caudal direction, coincided temporally with the appearance of somites during embryonic days 8.5-10.5. Somites form in a pairwise fashion within the presomitic mesoderm (PSM) following gastrulation. In the mouse embryo, somite pairs are laid down in a rostro-caudal progression with a total of 65 somite pairs formed during embryogensis. Somitogenesis is the basis of the segmented body plan and precursor to the axial skeleton, the dermis of the back, and all striated muscles of the adult body. Proteins proposed to participate in somitogenesis include c-hairy-1, notch/delta, and the eph family (30-33). The function of c-hairy-1 is suggested to be that of a molecular clock determining vertebrate segmentation as a result of transient waves of expression in chicken PSM that move rostrally with a periodicity corresponding to the time required to form one somite (90 min). A caudal-rostral wave of c-hairy-1 expression is repeated during the formation of each somite.

The notch/delta family was initially identified as a group of genes encoding cell-surface proteins that define neuronal cell fate and subsequently demonstrated to participate in prefiguring somite units. Notch/delta is expressed in a metaric pattern in the PSM, thereby establish boundaries of each somite segment during somitogenesis (39-42). Unlike c-hairy-1 or notch/delta mRNAs,

mARL4 mRNA was evenly distributed in each somite pair. Its appearance moves caudally as the embryo develops, as does the pattern of eph family signaling in somitogenesis (34). No other GTPase has apparently been implicated in somitogenesis. It will be important to investigate a possible link between the eph receptor tyrosine kinase family and the ARL small GTPase family in signal transduction pathways that determine cell fate during embryogenesis.

mARL4 mRNA was detected in the embryonic central nervous system at the earliest time examined (8.5-dpc mouse embryo), around the junction between the forebrain and mid brain. In 9.5-dpc mouse embryos, that earlier concentration of mARL4 had disappeared, and mARL4 was, instead, localized at the midbrain-hindbrain junction (Fig. 2). We interpret this change to mean that mARL4 may play a role in the establishment of central nervous system compartmentalization analogous to its function in the segmentation of somitogenesis. Indeed, Ephrin-A1, Ephrin-B2, and the receptor EphA4 are expressed in an iterative manner in the developing somites and in a gradient along the anterior-posterior axis of the developing midbrain (16, 34).

At later stages of embryonic development, mARL4 was found in specific central nervous system, structures, which included the neopallial cortex (future neocortex), ventricular zone of the cerebrum, and the spinal cord. The expression zones exactly matched those of neuronal cell bodies (perikaryon), which contain abundant rough ER, ribosomes, vesicles, and inclusions that are thought of as regions of mRNA concentration. A more comprehensive study will be required to define precisely the subcellular localization of mARF4 in individual cells.

Compared to ARL1 and ARL3, ARL4 contains an additional C-terminal putative bipartite NLS, i.e., K^{188}RRKMLRQQKKKR^{200} (Fig. 5A). Importin-α (karyopherin-α) is a protein of 530 amino acids that interacts directly with NLS. The C-terminal region of importin α recognizes the NLS-containing protein (35). Interaction of hARL4 with importin-α apparently depends on its C-terminal NLS, since ARL4-dC lacking 11 amino acids at the C-terminus failed to induce β-

galactosidase in the yeast two-hybrid assay. hARL4 interacted with five different recombinant importin-α constructs (residues 1-530, 135-530, 152-530, 233-530, and 235-530), each of which contains the NLS binding site in the C-terminal region. The *in vitro* interaction experiments using GTPase-defective (ARL4-Q79L) and GTP-binding defective (ARL4-T34N) mutants of ARL4, as well as ARL4-dC, confirmed that interaction of hARL4 with importin-α is not GTP-dependent and does require its C-terminal NLS.

Immunofluorescence microscopy and subcellular fractionation analyses revealed that endogenous mARL4 of Sertoli TM4 and neuroblastoma Neuro-2a cells was localized mainly in nuclei, in a punctate pattern (Fig 4). Although, transiently expressed GFP-ARL4 fusion protein was reported to be localized in nuclei (11), we found that some of the transiently expressed GFP-ARL4 was localized to nucleoli. Moreover, nucleolar concentration of ARL4-T34N appeared to depend on its GDP-bound conformation, since ARL4-Q-79L was not similarly concentrated. The function of the nucleolus as a factory for assembling ribosomal subunits is well established, but one of the more surprising findings of the past decade is the discovery of a variety of macromolecules in the nucleolus with no apparent ribosomal function(reviewed in Refs. 36 and 37). The nucleolus also seems to play a role in nuclear export, sequestering regulatory molecules, modifying small RNAs, assembling ribonucleoprotein (RNP), and controlling aging. In these novel events, the nucleolus serves as a privileged site for both recruitment and exclusion of regulatory complexes. The nucleolus may serve as a "sequestration center" for proteins that are to be kept inactive. This notion raises the possibility that some of the many proteins that have been localized to the nucleolus may be stored there in anticipation of eventual release. Interestingly, a $p34^{cdc2}$ homolog was localized to the nucleoli of neurons and glia in the mitotically quiescent murine central and peripheral nervous systems (38). Recently, three cell-cycle regulators, Cdc 14, Mdm2, and Pch2, have been identified whose activity is regulated by sequestration in nucleolus (reviewed in Ref. 39). Furthermore, nucleolar localization of the tumor suppressor protein p19ARF, with concomitant sequestration of the p53 inhibitor Mdm2, is disrupted by tumor-associated mutations and may be key for p53

activation (reviewed in Ref. 36). To our knowledge, ARL4 may be the first small GTPase reported to be localized in nucleoli. Although, the physiological significance of the presence of ARL4 in nucleoli is not understood, it will be important to determine whether ARL4 can participate in the regulation of nucleolar sequestration of proteins.

Of eight proteins that interacted with hARL4 in the yeast two-hybrid screening, one that interacted with ARL4-Q79L, but not ARL4WT or ARL4-T34N, in the two-hybrid system is the Sec7-domain of a known guanine nucleotide-exchange protein (GEP) (Liao et al., unpublished data). It will be interesting to learn whether this GEP, although believed to have an extra-nuclear distribution, can translocate into nuclei to activate ARL4. Six of the proteins that interacted with ARL4 have a nuclear localization and one of these is involved in the dynamics of the inner nuclear membrane and lamina (Liao et al., unpublished data). The small GTPase Ran, which plays a key role in nuclear transport, was recently reported to function also in mitosis by regulating microtubule nucleation and/or growth (40). The nuclear envelope of higher eukaryotes is a dynamic structure that breaks down during mitotic prometaphase and reforms during anaphase and telophase (41). During nuclear envelope breakdown, the nuclear lamina and pore complexes disassemble, and the nuclear membranes vesiculate. During reassembly, nuclear membranes are targeted to the daughter chromosomes where they fuse to enclose the chromatin. The nucleus then grows by protein import through newly assembled pore complexes and the fusion of additional vesicles. Our studies demonstrated that ARL4, like ARFs, can be amino-terminally myristoylated, consistent with a function dependent upon its reversible association with specific intracellular membranes that is influenced by myristoylation as well as guanine nucleotide binding. It has been suggested that a non-ARF GTPase is required for nuclear fusion and mitotic membrane disassembly (42), and we also speculate that ARL4 may have such a role in novel nuclear membrane trafficking and/or signaling cascades during embryonic development.

Acknowledgments: We thank Drs. Tang K. Tang and Shwu-Fen Chang for providing us with Sertoli cell (TM4) and Leydig cell (MA10) lines, Dr. H. Shih (at NHRI) for providing two-hybrid strains, plasmids, and library, and Dr. Ian Okazaki (NIH) for providing the rat testis RNA blot. This work was supported by grants from the National Science Council, R.O.C. (NSC-88-2318-B-002-005-M51) and partly by Yung-Shin Biomedical Research Fund (YSP-86-019) to F.-J. S. Lee, and by an internal fund of the National Taiwan University Hospital (NTUH-89A017) to P.-H. Huang and F.-J. S. Lee. We thank Drs. M. Vaughan, R. Haun and S.-M. Hsu for critical comments on the manuscript.

NOTE: Liao W.-L, Lin C-Y, Kuo J.-C., Moss J., and Lee F.-J. S. unpublished data.

REFERENCES

1. Moss, J., and Vaughan, M. (1998) *J. Biol. Chem.* **273,** 21431-21434
2. Boman, A. L., and Kahn, R. A. (1995) *Trends Biochem. Sci.* **20,** 147-150
3. Clark, J., Moore, L., Krasinskas, A., Way, J., Batttey, J., Tamkun, J., and Kahn, R. A. (1993) *Proc. Natl. Acad. Sci. USA* **90,** 8952-8956
4. Schurmann, A., Breiner, M., Becker, W., Huppertz, C., Kainulainen, H., Kentrup, H., and Joost, H.-G. (1994) *J. Biol. Chem.* **269,** 15683-15688
5. Cavenagh, M. M., Breiner, M., Schurmann, A., Rosenwald, A. G., Terui, T., Zhang, C.-j., Randazzo, P. A., Adams, M., Joost, H.-G., and Kahn, R. A. (1994) *J. Biol. Chem.* **269,** 18937-18942
6. Zhang, G.-F., Patton, W. A., Lee, F.-J. S., Liyanage, M., Han, J.-S., Rhee, S. G., Moss, J., and Vaughan, M. (1995) *J. Biol. Chem.* **270,** 21-24
7. Hong, J.-X., Lee, F-J. S., Patton, W. A., Lin, C.-Y., Moss, J., and Vaughan, M. (1998) *J. Biol. Chem.* **273,** 15872-15876
8. Lowe, S. L., Wong, S. H., and Hong, W. (1996) *J. Cell Sci.* **109,** 209-220
9. Lee, F.-J. S., Huang, C.-F., Yu, W.-L., Buu, L.-M., Lin, C.-Y., Huang, M.-C., Moss, J., and Vaughan, M. (1997) *J. Biol. Chem.* **272,** 30998-31005
10. Jacobs, S., Schurmann, A., Becker, W., Bockers, T. M., Copeland, N. G., Jenkins, N. A., and Joost, H. G. (1998) *Biochem J* **335,** 259-265
11. Jacobs, S., Schilf, C., Fliegert, F., Koling, S., Weber, Y., Schurmann, A., and Joost, H.-G. (1999) *FEBS let.* **456,** 384-388
12. Lee, F.-J. S., Stevens, L. A., Kao, Y. L., Moss, J., and Vaughan, M. (1994) *J. Biol. Chem.* **269,** 20931-20937
13. Sanger, F., Nicklen, S., and Coulson, R. A. (1977) *Proc. Natl. Acad. Sci. USA* **74,** 5463-5467

14. Carson, D. D., Rosenberg, L. I., Blaner, W. S., Kato, M., and Lennarz, W. J. (1984) *J. Biol. Chem.* **259,** 3117-3123

15. Ascoli, M. (1981) *Endocrinology* **108,** 88-95

16. Cheng, H.-J., Nakamoto, M., Bergemann, A. D., and Flanagan, J. G. (1995) *Cell* **82,** 371-381.

17. Cheng, H.-J., and Flanagan, J. G. (1994) *Cell* **79,** 157-168

18. Hong, J.-X., Haun, R. S., Tsai, S.-C., Moss, J., and Vaughan, M. (1994). *J. Biol. Chem.* **269,** 9743-9745

19. Harlow, E., and Lane, D. (1988) Antibodies: A Laboratory Manual. Cold Spring Harbor Laboratory, Cold Spring Harbor, New York.

20. Yang, C. Z., Heimberg, H., D'Souza-Schorey, C., Mueckler, M. M., and Stahl, P. D. (1998). *J. Biol. Chem.* **273,** 4006-4011

21. Schreiber, E., Matthias, P., Muller, M. M., and Schaffner, W. (1989) *Nucleic Acids Res.* **17,** 6419

22. Dascher, C., and Balch., W. E. (1994) *J. Biol. Chem.* **269,** 1437-1448

23. Hollenberg, S. M., Sternglanz, R., Cheng, P. F., and Weintraub, H. (1995) *Mol. Cell. Biol.* **15,** 3813-3822

24. Ito, H., Fukuda, Y., Murata, K., and Kimura, A. (1983) *J. Bacteriol.* **153,** 163-168

25. Haun, R. S., Tsai, S.-C., Adamik, R., Moss, J., and Vaughan, M. (1993) *J. Biol. Chem.* **268,** 7064-7068

26. Huang, C.-F., Buu, L.-M., Yu, W.-L., and Lee, F.-J. S., (1999) *J. Biol. Chem.* **274,** 3819-3827.

27. Northup, J. K., Sternweis, P. C., and Gilman, A. G. (1983) *J. Biol. Chem.* **258,** 11361-11368

28. Cuomo, C. A., Kirch, S. A., Gyuris, J., Brent, R., and Oettinger, M. A. (1994) *Proc. Natl. Acad. Sci. USA* **91,** 6156-6160

29. Weis, K., Mattaj, I. W., and Lamond, A. I. (1995) *Science* **268,** 1049-1054

30. Palmeirim, I., Henrique, D., Ish-Horowicz, D., and Pourquie, O. (1997) *Cell* **91,** 639-648

31. Izpisua-Belmonte, J. C., De Robertis, E. M., Storey, K. G., and Stern, C. D. (1993) *Cell* **74,** 645-659

32. Conlon, R. A., Reaume, A. G., and Rossant, J. (1995) *Development* **121,** 1533-1545

33. Hrabe de Angelis, M., McIntyre, J. 2nd., and Gossler, A. (1997) *Nature* **386,** 717-721

34. Durbin, L., Brennan, C., Shiomi, K., Cooke, J., Barrios, A., Shanmugalingam, S., Guthrie, B., Linberg, R., and Holder, N. (1998) *Genes Dev.* **12,** 3096-3109

35. Moroianu, J., Blobel, G., and Radu, A. (1996) *Proc. Natl. Acad. Sci. USA* **93,** 6572-6576

36. Garcia, S. N., Pillus, L. (1999) *Cell* **97,** 825-828

37. Olson, M. O., Dundr, M., and Szebeni, A. (2000) *Trends Cell Biol.* **10,** 189-196

38. Ino, H., Mochizuki, T., Yanaihara, N., and Chiba, T. (1993) *Brain Res.* **614,** 131-136

39. Visintin, R., and Amon, A. (2000) *Curr. Opin. Cell Biol.* **12,** 372-377

40. Heald, R., and Weis, K. (2000) *Trends Cell Biol.* **10,** 1-4

41. Gant, T. M., and Wilson, K. L. (1997) *Annu Rev Cell Dev Biol* **13,** 669-695

42. Gant, T. M., and Wilson, K. L. (1997) *Eur. J. Cell Biol.* **74,** 10-19

FIGURE LEGENDS

FIG. 1. ARL4 mRNA in mouse tissue and embryos and rat testis. Blots containing poly $(A)^+$ RNA from adult mouse tissues (A) or whole embryos at different developmental stages (B) were hybridized with a random-primed, ^{32}P-labeled mARL4 cDNA probe. Hybridization with a β-actin probe was a control for sample loading. (C) A blot containing poly $(A)^+$RNA (2μg) from prepubertal (5 and 10 days), early pubertal (15 days), midpubertal (20 and 25 days), late pubertal (30 days), and adult (60 days) rat testis was hybridized with a random-primed, ^{32}P-labeled rat ARL4 cDNA probe and a GAPDH cDNA as control.

FIG. 2. *In situ* RNA hybridization of mARL4 in day 8.5 – day 9.5 mouse embryos. Embryos at day-8.5 at the 10-12 somite stage (A), day-9.0 at the 15-20 somite stage (B), and day-9.5 at the 25-29 somite stage (C) were hybridized with the mARL4 antisense probe or (D) with the sense probe. Structures that appear to show specific reactivity include forebrain-midbrain junction (black arrow); somites (red arrows) and midbrain-hindbrain junction (arrowhead).

FIG. 3. *In situ* hybridization of ARL4 mRNA in mouse embryos at day14.5-17.5 pc. Pairs of sections of each embryo were reacted with the mARL4 antisense probe (A-C) or stained with hematoxylin-eosin (D-F). Day-14.5 embryo (A, D) is a transverse section near the level of the nasopharnyx. Structures that appear to show specific reactivity include neuronal stoma around the central canal of the spinal cord (arrows), the dorsal horn (arrowheads), the ventral horn (asterisks) and the root ganglion (red arrow head). Abbreviations are: c.p., cartilage primordium; c.a., common carotid artery; e, esophagus; l, larynx. Day-16.5 embryo (B, E) is a sagittal section. The root ganglion (red arrowhead) and spinal cord (arrows) show mARL4 reactivity. Abbreviations are: Int, intestine; Liv, liver; Kid, kidney. Day-17.5 embryo (C, F) is a coronal

section through the head. Generalized mARL4 reactivity in the brain parenchyma is detected, especially in the neopallial cortex (arrows).

FIG. 4. Immunolocalization of endogenous mARL4 in Sertoli TM4 and neuroblastoma Neuro-2a cells. (A) Specificity of antibody against ARL4. ~100 ng of the indicated purified recombinant His-tagged ARL (a and b) and the indicated amounts of purified His-tagged mARL4 (c) were subjected to SDS-PAGE in 12.5 % gels. Proteins were transferred to nitrocellulose and reacted with (a) anti-His-tag or (b and c) anti-ARL4 antibodies, followed by detection using the ECL system (A, B). (B) Subcellular distribution of mARL4. Nuclear (N), membrane (M), and cytosolic (C) fractions of Sertoli TM4 cells were prepared as described in Materials and Methods. Equivalent amounts (from total homogenate) of each fraction were analyzed by electrophoresis and immunoblotting using specific antibodies against ARL4, α-tubulin (cytosolic marker), or PCNA (nuclear marker). The lowest panel shows results of immunoprecipitation using specific anti-ARL1 serum (7); positions of ARL1 and the light chain of IgG are marked. Positions of protein standards (kDa) are on the left. (C) Immunolocalization of ARL4. Sertoli TM4 or neuroblastoma Neuro-2a cells on glass coverslips, treated as described in Materials and Methods, were incubated with primary antibodies, the affinity-purified anti-hARL4-peptide (a, i), or the same antibodies after incubation with purified hARL4 (e), and mouse anti-β-COP (c, g, and k). Coverslips were mounted on Mowiol (supplemented with Hoescht 33258, b, f, and j) and inspected with a Zeiss Axiophot equipped for epifluorescence. Phase contrast microscopy (d, h, and l) views are on the right. (D) Immunohistochemical localization of mARL4 protein in coronal section of 14-dpc mouse embryo. Immunohistochemistry was performed using an avidin-biotin system, the ABC Vectastain Elite kit (Vector Laboratories, Burlingame, CA) as described in Materials and Methods. The spinal cord (arrow heads), root trunks (arrows), and sclerotome (stars) are indicated.

FIG. 5. Interaction of hARL4 with importin α in the two-hybrid system. (A) Diagramatic comparison of wild type (WT) hARL1, hARL3, and hARL4 and three hARL4 mutants with the total number amino acids on the right. Residues 188 to 200 contain the bipartite NLS of ARL4. ARL-dC lacks 11 of those amino acids (190 to 200) at the C-terminus. Positions of the mutations Q79L and T34N are also indicated. (B) Expression of LexA-ARL fusion proteins. Yeast reporter strain L40 was transformed with the indicated LexA construct, pBTM116 (LexA only), or pLexA-lamin. Samples (~20 μg) of cell lysates were subjected to SDS-PAGE in a 10 % gel. Proteins were transferred to nitrocellulose and reacted with anti-LexA antibodies (upper panel), or specific anti-ARL1 (16), anti-ARL3 (Liao et. al. unpublished data), or anti-ARL4 antibodies as indicated (lower panel), followed by detection using the ECL system. Positions of protein standards (kDa) are on the left. (C) Interaction of hARL4 and mutants with importin-α in the two-hybrid system. The yeast reporter strain L40 was co-transformed with pACT2-importin-α and the indicated pLexA-ARL construct or pLexA-lamin. Co-transformants were plated on synthetic histidine-containing medium lacking leucine, tryptophan, uracil, and lysine (His+ plate, upper panel). Colonies from His+ plates were assayed for β-galactosidase activity by a filter assay to test for specificity (lower panel). Colonies from His+ plates were also patched on His-minus selective plates lacking histidine, leucine, tryptophan, uracil, and lysine (His- plate, middle panel). (D) *In vitro* interaction of GST-importin-α with various hARL4 constructs. Recombinant His-tagged ARL4, ARL4-Q79L, ARL4-T34N, ARL4-dC, and ARL1 were synthesized in *E coli*, and 750 μl of soluble fraction from each batch of cells, as indicated, were incubated with 10 μg GST or GST-importin-α immobilized on glutathione-Sepharose beads at 4 °C for 1 h. After washing five times with ice-cold washing buffer, 25 μl of SDS sample buffer was added to each batch of beads, followed by boiling for 10 min. From each preparation, a sample (15 μl) of was subjected

to SDS-polyacrylamide electrophoresis in 12% gel. A sample (7.5 μl) of the indicated *E. coli* soluble fraction, in the first lane, is followed by GST-bound and GST-importin-α-bound samples in each group of three lanes.

FIG. 6. Transient Expression of hARL4 and its Mutants in COS7 Cells. (A) Localization of hARL4 and mutants in COS7 cells. Cells transfected with GFP fusion constructs of ARL4, ARL4-Q79L, ARL4-T34N, and ARL4-dC were grown on glass coverslips, fixed with formaldehyde, incubated with primary antibodies, mouse anti-p58 (Golgi marker) (d, h, l, and p) or mouse anti-nucleolin (nucleolar marker) (t). Coverslips were mounted on Mowiol (supplemented with Hoescht 33258, b, f, j, n, and r) and inspected with a Zeiss Axiophot equipped for epifluorescence. Phase contrast microscopy (a, e, i, m, and q) and GFP-ARL4 fluorescence (c, g, k, o, and s; green) are shown. (B) Subcellular distribution of ARL4. Nuclear fraction (N), membrane (M), and cytosolic (C) fractions of COS7 cells were prepared as described in Materials and Methods. Equivalent amounts (from total homogenate) of each were analyzed by immunoblotting analysis using specific antibodies against ARL4, α-tubulin (cytosolic marker) and PCNA (nuclear marker).

FIG. 7. Effects of phospholipids on GTPγS binding to hARL4. Samples of recombinant hARF1, hARL1, or hARL4 (3 μg) plus 0.15 μg/μl cardiolipin (CL), 0.2 μg/μl phosphatidylserine (PS), or 0.015 μg/μl phosphatidylcholine (PC), as indicated, were incubated with 4 μM GTPγS at 30°C for 1 h. Data are the means of values from triplicate assays plus/minus one-half the range. Data are representative of at least two separate experiments.

FIG. 8. Expression of myristoylated hARL4. Recombinant hARL4, hARL1, and yARL3 were synthesized in *E. coli* co-expressing yeast *N*-myristoyltransferase and grown in medium containing (^{3}H)-myristic acid. Samples of bacterial proteins (~20 μg) were subjected to SDS-PAGE in a 15% gel. Upper panel: gel fixed in 10% acetic acid and 45% methanol for 30 min, incubated in Amplify (Amersham) for 20 min, dried, and exposed to Hyper-film (Amersham) for 41 h at -80°C. Lower panel: nitrocellulose blot of the three recombinant proteins after SDS-PAGE was reacted with antibodies against ARL4, hARL1 (16), or yeast ARL3 (34); and the ECL system was used for visualization.

Table I

Oligonucleotides used in the analysis of ARL4

Name	Sequence (5' -------> 3')
ARL-R1	T/C-T-C-T/C-T-G-A/C/G/T- C-C-ACGT-C-C-A/C/G/T-A-C-A/G-T-C-C-C-A
ARL-R2	T/C-T-T-C-C-A-A/C/G/T-A-A/G-A/C/G/T-G-G-A/C/G/T-C-G/T-A/C/G/T-A-A/G-C/T-T-T
ARL4A	GAATTC GGG AAT GGG CTG TCA GAC CAG[a]
ARL4B	TCT AGA TCT TTT CTT TTT CTG TTG CCG CAA[b]
ARL4C	TC TGG GAT GTA GGT GGT CTG GAG AAA TTA AGG CCA CT[c]
ARL4D	AG TGG CCT TAA TTT CTC CAG ACC ACC TAC ATC CCA GA[c]
ARL4E	TG GAC TGT GCT GGA AAG AAC ACT GTC TTA TAC AGG CT[d]
ARL4F	AG CCT GTA TAA GAC AGT GTT CTT TCC AGC ACA GTC CA[d]
ARL4G	TCT AGA TCT TTT CTT TTT CTG TTG CCG[b]

[a] Underlined bases introduce *EcoR*I site. [b] Underlined bases introduce *Xba*I site. [c] Underlined base introduces Q79L point mutation. [d] Underlined bases introduced T34N point mutation.

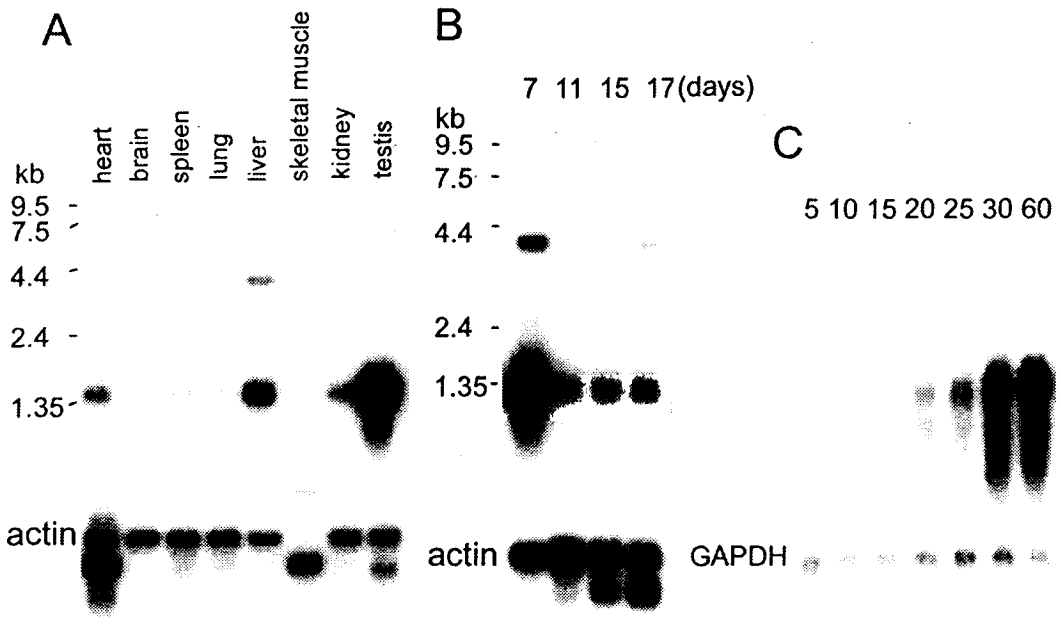
A
heart
brain
spleen
lung
liver
skeletal muscle
kidney
testis
kb
9.5
7.5
4.4
2.4
1.35
actin
B
7 11 15 17(days)
kb
9.5
7.5
4.4
2.4
1.35
actin
C
5 10 15 20 25 30 60
GAPDH

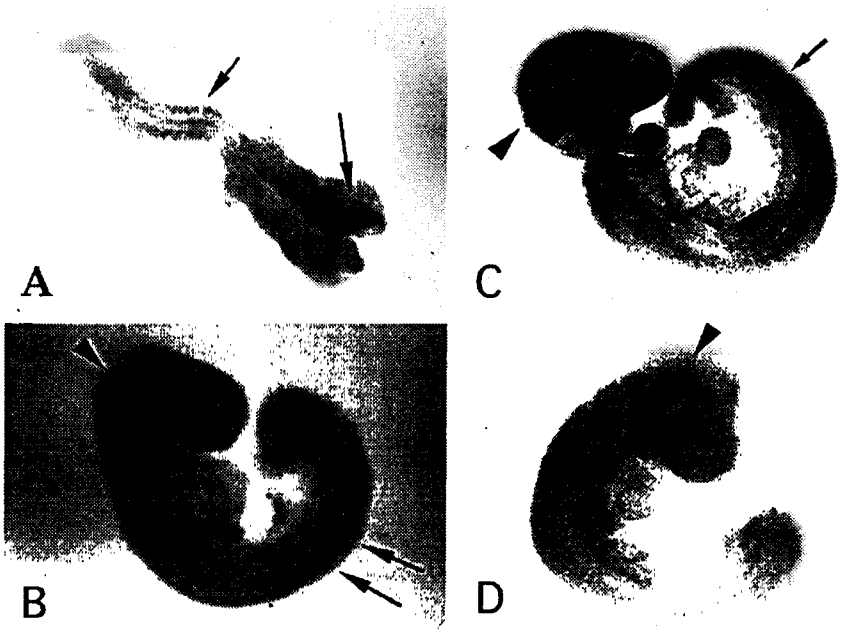
A
C
B
D

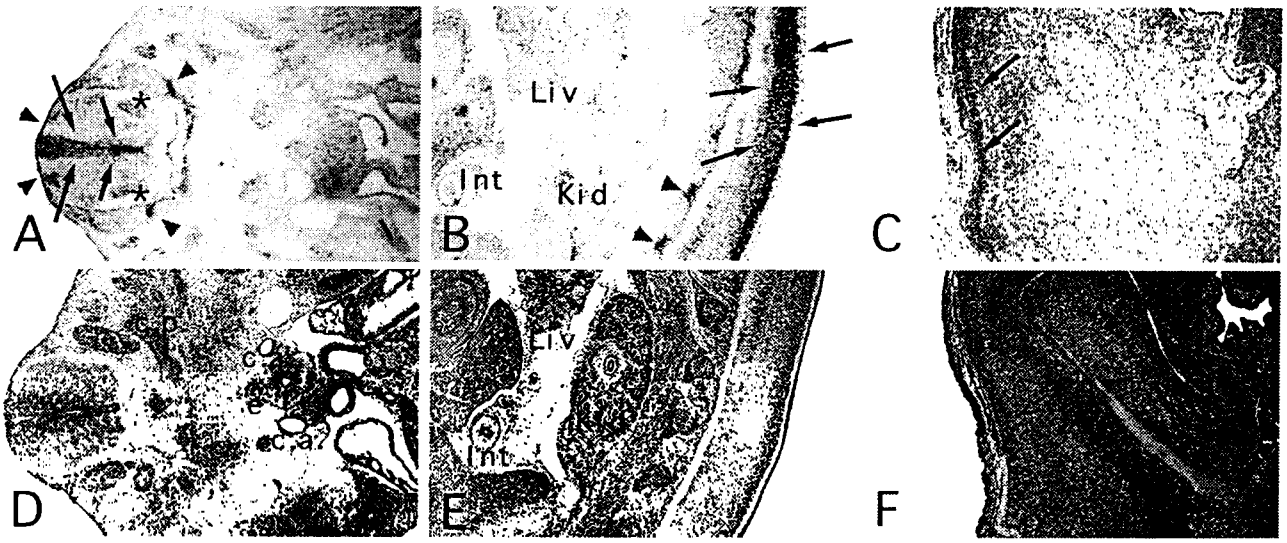
A
B
Liv
Int
Kid
C
D
E
Liv
Int
F

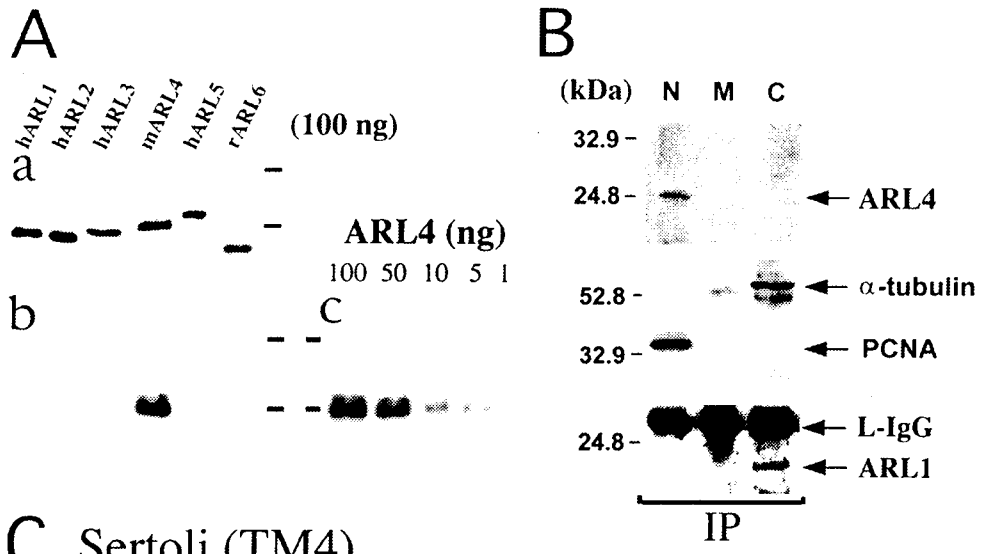
A
hARL1
hARL2
hARL3
mARL4
hARL5
rARL6
(100 ng)
a
ARL4 (ng)
100 50 10 5 1
b
c
B
(kDa) N M C
32.9
24.8
ARL4
52.8
α-tubulin
32.9
PCNA
24.8
L-IgG
ARL1
IP

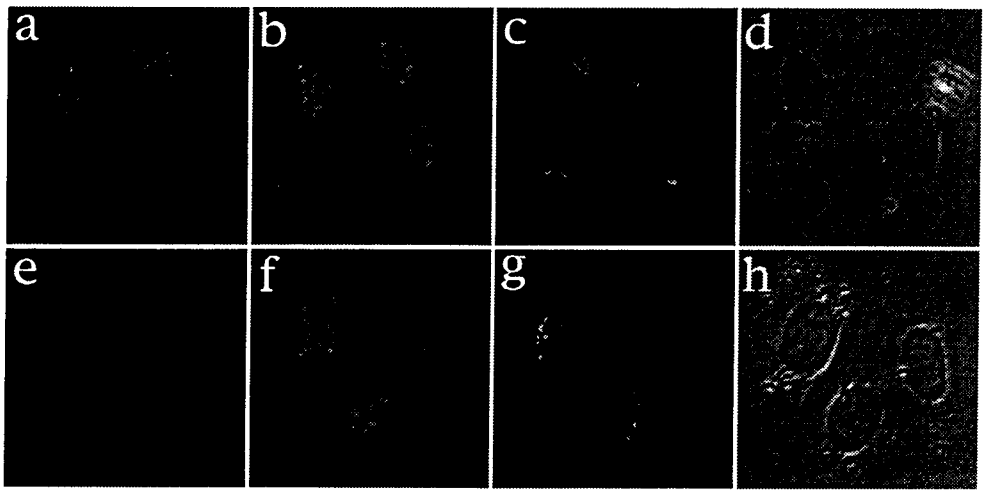
C Sertoli (TM4)
a
b
c
d
e
f
g
h

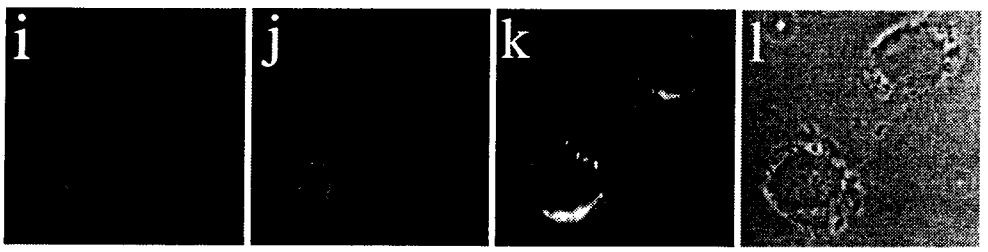
Neuroblastoma (Neuro-2a)
i
j
k
l

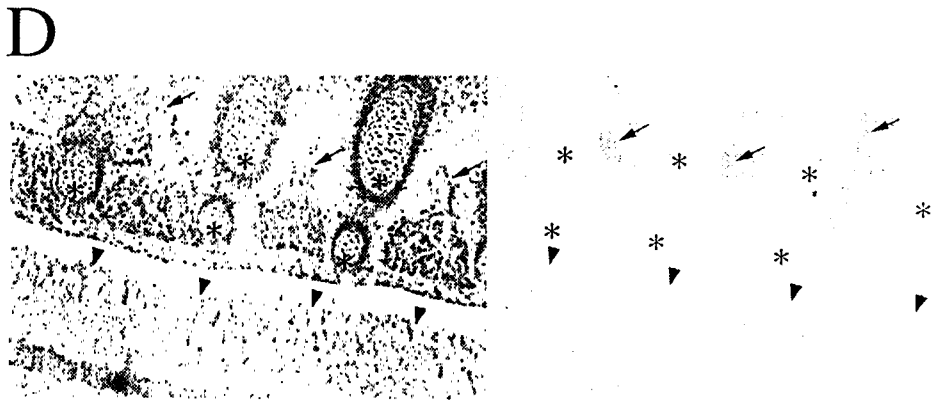
D

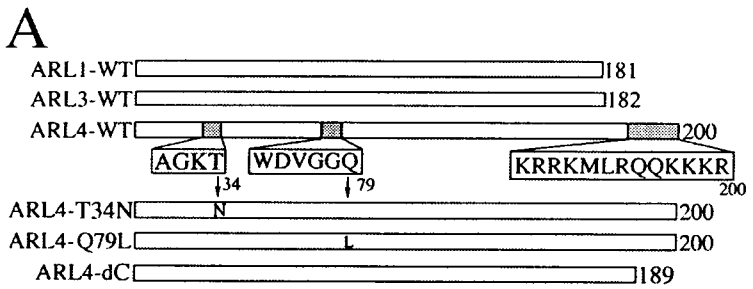
A
ARL1-WT
181
ARL3-WT
182
ARL4-WT
200
AGKT
WDVGGQ
KRRKMLRQQKKKR
34
79
200
ARL4-T34N
N
200
ARL4-Q79L
L
200
ARL4-dC
189

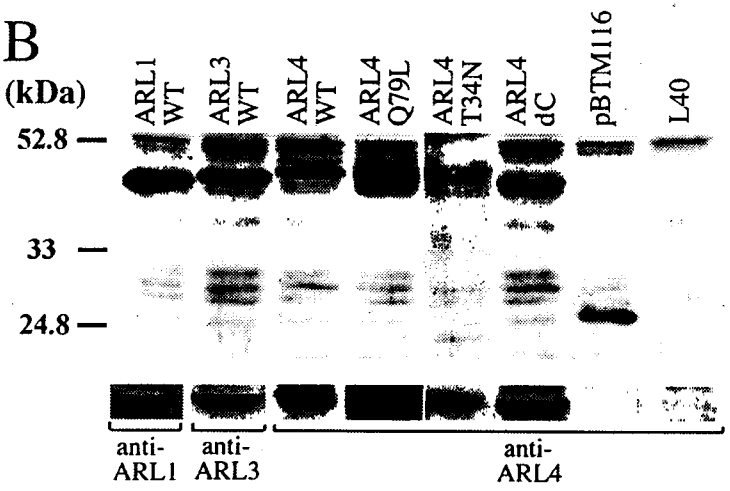
B
(kDa)
ARL1 WT
ARL3 WT
ARL4 WT
ARL4 Q79L
ARL4 T34N
ARL4 dC
pBTM116
L40
52.8
33
24.8
anti-ARL1
anti-ARL3
anti-ARL4

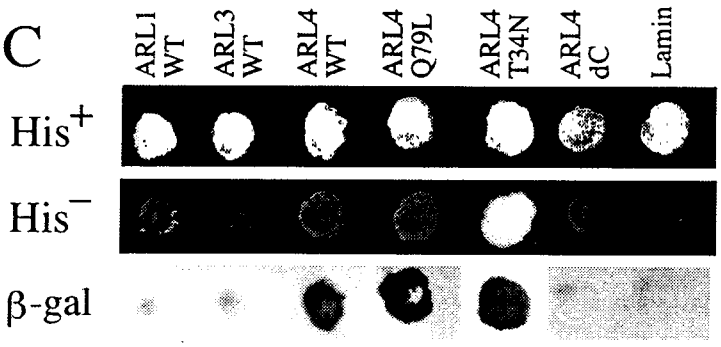
C
ARL1 WT
ARL3 WT
ARL4 WT
ARL4 Q79L
ARL4 T34N
ARL4 dC
Lamin
His+
His−
β-gal

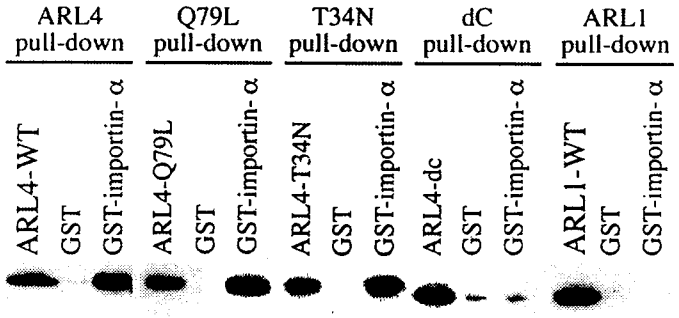
D
ARL4 pull-down
Q79L pull-down
T34N pull-down
dC pull-down
ARL1 pull-down
ARL4-WT
GST
GST-importin-α
ARL4-Q79L
GST
GST-importin-α
ARL4-T34N
GST
GST-importin-α
ARL4-dc
GST
GST-importin-α
ARL1-WT
GST
GST-importin-α

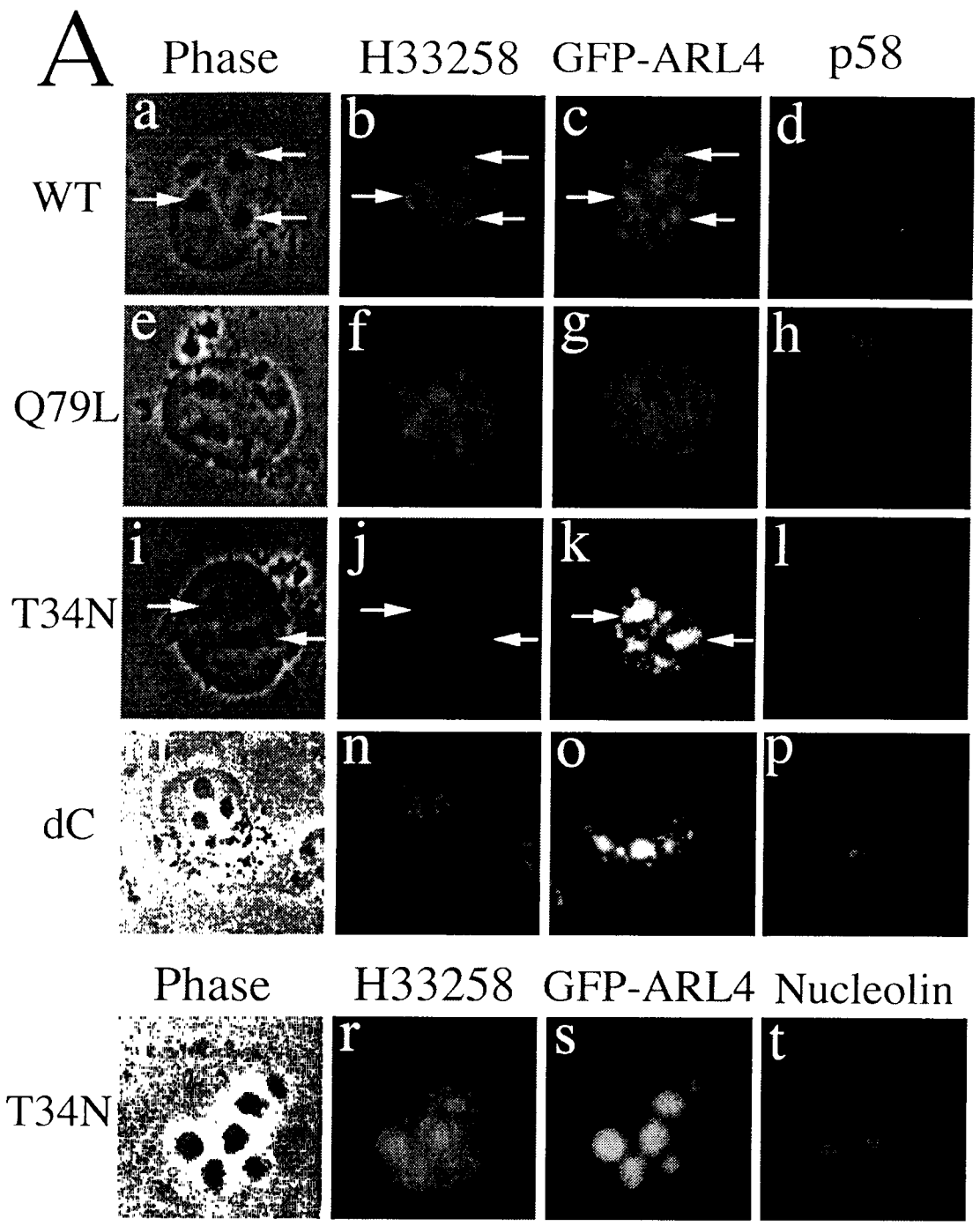
A
Phase
H33258
GFP-ARL4
p58
WT
Q79L
T34N
dC
a
b
c
d
e
f
g
h
i
j
k
l
n
o
p
Phase
H33258
GFP-ARL4
Nucleolin
T34N
r
s
t

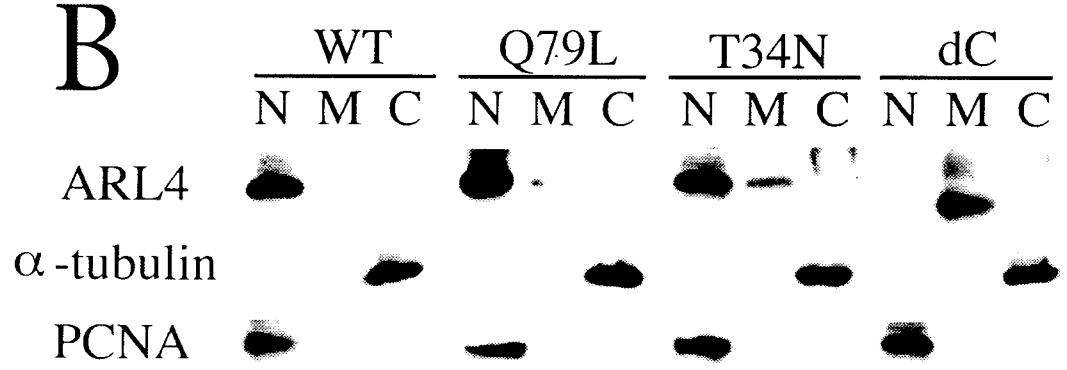
B
WT
Q79L
T34N
dC
N M C N M C N M C N M C
ARL4
α-tubulin
PCNA

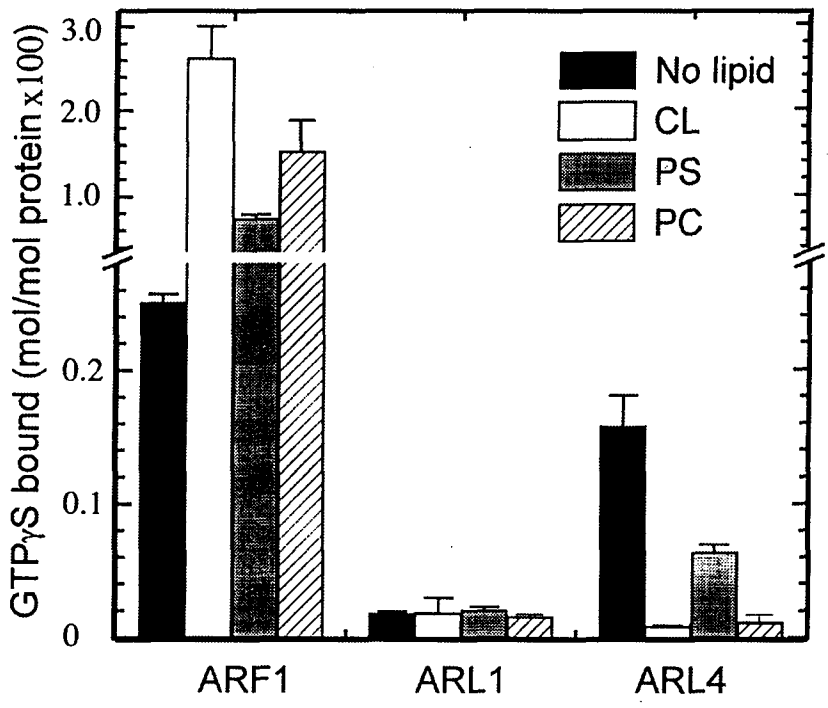
GTPγS bound (mol/mol protein x100)
3.0
2.0
1.0
0.2
0.1
0
No lipid
CL
PS
PC
ARF1
ARL1
ARL4

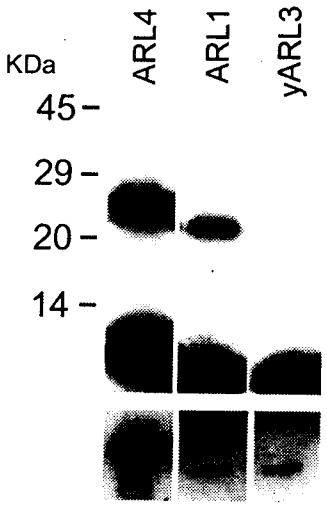
KDa
ARL4
ARL1
yARL3
45
29
20
14